

Transient hydrodynamic phonon transport in two-dimensional disk geometry

Chuang Zhang^{1,*} and Lei Wu^{1,†}

¹*Department of Mechanics and Aerospace Engineering,
Southern University of Science and Technology, Shenzhen 518055, China*

(Dated: March 25, 2022)

This paper is a continuation of our work on the transient hydrodynamic phonon transport from three-dimensional to two-dimensional materials. In the previous work [Zhang *et al.*, *Int. J. Heat Mass Transfer* 181, 121847 (2021)], a transient heat conduction phenomenon proving the existence and uniqueness of hydrodynamic phonon transport in three-dimensional materials was found, namely, using a heating laser pulse to heat the materials under the environment temperature, after the heating laser is removed, the transient temperature could be lower than the environment temperature. Whether this phenomenon could appear in two-dimensional materials needs further study. In this paper, the transient heat conduction in two-dimensional disk geometry is studied based on the phonon Boltzmann transport equation (BTE). Our results show that this phenomenon could appear in two-dimensional disk geometry and only appear in the hydrodynamic regime. In addition, the possibility of this phenomenon observed by experiments is theoretically discussed by using the experimental parameters as the input of the phonon BTE. Results show that this phenomenon could appear in a single-layer suspended graphene disk with diameter $7\ \mu\text{m}$ in the temperature range of $50 - 150\ \text{K}$. The present work could provide theoretical guidance for the future experimental proof of hydrodynamic phonon transport in two-dimensional materials.

I. INTRODUCTION

Hydrodynamics is a kind of macroscopic phenomenon¹⁻⁴, resulting from the frequent interactions between microscopic (quasi-)particles and satisfying the conservation principles of physical quantities, including mass, momentum and energy. Compared to the ubiquitous fluid hydrodynamics phenomena in our daily life, the observation of hydrodynamics behaviors in solid materials is much more difficult because the momentum is usually broken during phonon scattering processes^{5,6}.

In order to observe the phonon hydrodynamics phenomena in solid materials, the momentum of the thermal system must be highly conserved, which requires that the momentum conserved N-process should be much sufficient and meanwhile the R-process should be rare or insufficient⁷⁻¹¹. In the early days, the phonon hydrodynamics phenomenon could only be observed experimentally in a few three-dimensional materials and at sufficiently low temperatures (near $10\ \text{K}$)¹²⁻¹⁷, which significantly limited its further development and research. Fortunately, this dilemma was broken in the recent seven years^{5,6}. In 2015, researchers found that the N-process in suspended graphene is much more sufficient than the R-process, and the drifting second sound could be predicted theoretically at $100\ \text{K}$ ¹⁸. This seminal work sets off an upsurge of theoretical and experimental research on phonon hydrodynamics phenomena in low-dimensional or multi-layer materials, such as the drifting second sound¹⁹⁻²¹, heat vortices²² and phonon Poiseuille flow with parabolic distribution of heat flux²³⁻²⁵. The drifting second sound, more specifically, the temperature wave signal was measured experimentally by the transient thermal

grating method in high-quality graphite samples at $100 - 200\ \text{K}$ ^{26,27}. Until now, the parabolic distribution of heat flux or the heat vortices has never been measured directly in experiments. The Knudsen minimum phenomenon and temperature dependent thermal conductivity, which increases faster than that in the ballistic limit²⁸⁻³⁰, are usually regarded as the indirect macroscopic evidences of the phonon Poiseuille flow.

Above thermal behaviors have usually been regarded as the macroscopic signatures of the hydrodynamic phonon transport with sufficient N-process in previous studies^{5,26,27}. However, some studies have also reported that the temperature wave phenomenon could appear even if the N-process is insufficient³¹⁻³⁴. According to Hardy's work³⁵, when the all phonons have similar relaxation time and there are external time-dependent heat sources whose heating period is comparable to the phonon relaxation time, the driftless second sound could appear. And the drifting and driftless second sound have the same propagation speed at the macroscopic level when the linear phonon dispersion is accounted. Based on first-principle and linearized phonon BTE, Cepellotti *et al.* found that the driftless second sound can appear in two-dimensional materials even under the normal condition³⁶. Recently, the temperature wave signal was measured by the frequency-domain thermoreflectance experiments in room temperature Germanium with insufficient N-process³². On the other hand, when the N-process is ignored, the heat vortices^{37,38} or the parabolic distribution of heat flux^{11,39} can also be predicted as long as the R-process is insufficient. In a word, when the temperature wave, heat vortices or the parabolic distribution of heat flux is observed at the macro-

scopic/experimental level, the sufficient N-process is not necessarily required or the phonon transport may not be in the hydrodynamic regime.

Hence, if we want to experimentally prove the existence and uniqueness of hydrodynamic phonon transport, one of the best way might be to find a macroscopic phenomenon that only appears when the N-process is very sufficient and meanwhile the R-process is very insufficient. For the steady problem, the Knudsen minimum phenomenon is an excellent candidate to prove the existence and uniqueness of hydrodynamic phonon transport although it is indirect^{23–25,29,30}. In homogeneous 2D and 3D hotspot systems, the temperature distributions in the radial direction are stratified in different phonon transport regimes⁴⁰, which may be another candidate. For unsteady problem, a novel transient heat conduction phenomenon was reported based on frequency-independent BTE in a recent paper⁴¹, namely, the transient temperature could be lower than the lowest value of initial temperature when the external heat source is removed. This phenomenon appears only when the N-process dominates heat conduction. It was also measured by picosecond laser irradiation in a highly oriented pyrolytic graphite in the temperature range of 80 – 120 K⁴². However, both of them focused on three-dimensional materials.

Therefore, our main goal in the present work is to figure out whether this transient phenomenon could appear in two-dimensional materials, and whether it only appears in the hydrodynamic regime. The rest of the paper is organized as follows. The physical problem is described in Sec. II and the phonon BTE is introduced in Sec. III. Results and discussions are shown in Sec. IV. Finally, conclusions are made in Sec. V.

II. PROBLEM DESCRIPTION

As shown in Fig. 1, in a two-dimensional disk geometry with diameter L , the initial environment temperature is T_0 . The outer of the disk is the heat sink with fixed temperature T_0 . When $t > 0$, a heating pulsed Gaussian laser beam with radius r_{pump} is added at the center and it continues to heat the system for a while. The temperature rise is controlled much small. When $t > t_h$, the heating pulse is removed and the temperature will dissipate with time gradually, where t_h is the heating time.

The transient heat conduction process can be described by

$$\frac{\partial E}{\partial t} + \nabla \cdot \mathbf{q} = \dot{S}(\mathbf{x}, t), \quad (1)$$

where E , \mathbf{q} and \dot{S} are the local energy, heat flux and the external heat source, respectively. All of

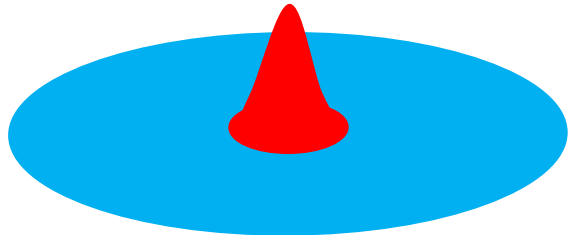


FIG. 1. Schematic of the 2D disk with a heat source at the center.

them depend on spatial position \mathbf{x} and time t . The heating pulsed Gaussian laser beam is

$$\dot{S} = \begin{cases} A \exp\left(-\frac{|\mathbf{x}-\mathbf{x}_c|^2}{r_{pump}^2}\right), & 0 < t < t_h \\ 0, & t \geq t_h \end{cases} \quad (2)$$

where \mathbf{x}_c and A are the center and peak of the heating pulse, respectively. In practical pump-probe experiments^{32,43,44}, the measured temperature is usually a Gaussian average over the spatial range of the probe pulse. Besides, the probe time is much shorter than the temperature decay time so that we ignore the average of the sampling time. In this work, we mainly focus on the temperature variance at the disk center so that the probe temperature is

$$T_{probe}(t) = \frac{\int T(\mathbf{x}, t) \exp\left(-\frac{|\mathbf{x}-\mathbf{x}_c|^2}{r_{probe}^2}\right) d\mathbf{x}}{\int \exp\left(-\frac{|\mathbf{x}-\mathbf{x}_c|^2}{r_{probe}^2}\right) d\mathbf{x}}, \quad (3)$$

where r_{probe} is the laser spot radius of the probe pulse and T is the local temperature. In addition, we set

$$T_h = T_{probe}(t_h). \quad (4)$$

Obviously, $T_{probe} < T_h$ when the heating pulse is removed.

III. PHONON BTE

The key of Eq. (1) is the constitutive relation between the heat flux and temperature. Unfortunately, the Fourier's law breaks down at the micro/nano scale. In order to correctly describe the multiscale transient heat conduction process, the phonon Boltzmann transport equation (BTE) under the Callaway approximation is used^{11,20,22,41,45,46},

$$\frac{\partial e}{\partial t} + v_g \mathbf{s} \cdot \nabla_{\mathbf{x}} e = \frac{e_R^{eq} - e}{\tau_R} + \frac{e_N^{eq} - e}{\tau_N} + \frac{\dot{S}}{2\pi}, \quad (5)$$

where e is the phonon distribution function of energy density, v_g is the group velocity and \mathbf{s}

is the unit directional vector in two-dimensional solid angle space. The phonons may suffer from different scattering processes before reaching associated steady-state distributions, including N-process, R-process and boundary scattering. The N-process conserves both energy and momentum, while the R-process only conserves energy. e_R^{eq} and e_N^{eq} are the associated phonon equilibrium distribution functions for R- and N- processes, respectively. τ_R and τ_N are the relaxation times for R- and N- processes, respectively. The local energy density, heat flux and temperature are obtained by taking the moments of the distribution function.

$$E = \sum_p \int \int e d\Omega d\omega, \quad (6)$$

$$T = T_0 + \frac{E}{\sum_p \int C d\omega}, \quad (7)$$

$$\mathbf{q} = \sum_p \int \int \mathbf{v} e d\Omega d\omega, \quad (8)$$

where the integral is conducted in both the solid angle space $d\Omega$ and frequency space $d\omega$, C is the spectral specific heat and p is the polarization. Note that the temperature cannot be well defined in non-equilibrium thermal systems, so that the temperature in this study is more like the symbol of local energy density⁴⁷. $\dot{s} = G\dot{S}$ is the spectral volumetric heat generation^{48,49}, and G is the associated weight satisfying

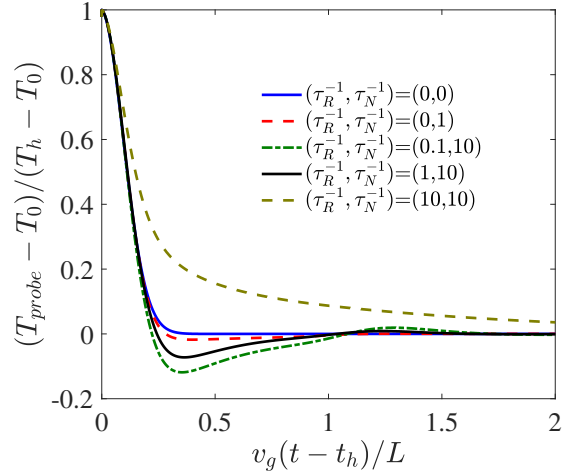
$$\sum_p \int G d\omega = 1. \quad (9)$$

In general, G is much complex and related to the actual physical nature of heat source^{48,50}. When phonon frequency ω and polarization p are not considered, $G = 1$. The thermalizing boundary conditions are used for the heat sink and all phonons emitted from the heat sink are the equilibrium distribution function $e_R^{eq}(T_0)$. More details of phonon BTE can refer to previous studies^{20,22,34,41,51}. In order to obtain the accurate numerical solutions of the phonon BTE, the discrete unified gas kinetic scheme⁵² and the implicit kinetic scheme are used, which can be found in our previous studies^{34,41}. The numerical discretizations of the whole phase space are shown in Appendix A.

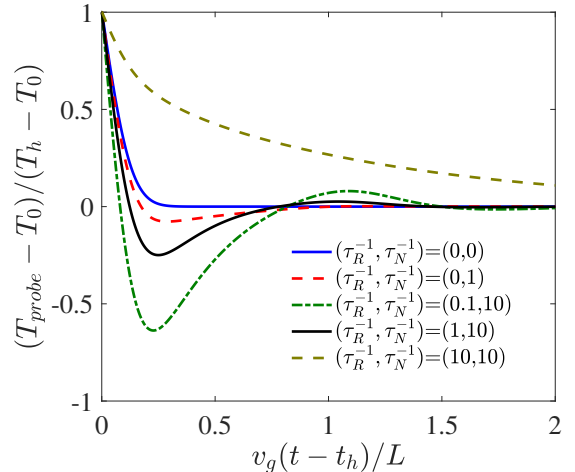
IV. RESULTS AND DISCUSSIONS

The transient heat conduction in 2D disk geometry with a fixed system size is simulated, and the Debye linear dispersion approximation and gray model are used^{11,22,41,46}. The heat conduction is not limited by specific materials properties and

all physical variables are dimensionless. We fixed $L = 1$, $r_{pump} = r_{probe} = 0.1$, $C = 1$ and $v_g = 1$.



(a) Ultra short heating time $v_g t_h/L = 0.01$



(b) Ultra long heating time $v_g t_h/L = 5.0$

FIG. 2. The evolution of temperature in 2D disk geometry.

The evolution of probe temperature are shown in Fig. 2 after the heat source is removed. It can be found that $(T_{probe} - T_0)/(T_h - T_0) \geq 0$ when rare phonon scattering happens. However, when the N-process is more sufficient than the R-process, the transient temperature could be smaller than the environment temperature when $v_g(t - t_h)/L < 0.45$. Furthermore, this phenomenon becomes more obvious with the increase of N-process. When the R-process increases, this phenomenon becomes weak and finally disappears. In addition, based on the results in Fig. 2(a)(b) with different heating time t_h , it can be found that the appearance of this phenomenon in the hydrodynamic regime is slightly affected by the heating time t_h of the laser beam.

The underlying physical mechanisms are discussed below. In the ballistic regime, phonons

transport with rare scattering so that

$$e(\mathbf{x}, \mathbf{s}, t + \delta t) = e(\mathbf{x} - v_g \mathbf{s} \delta t, \mathbf{s}, t), \quad t \geq t_h, \quad (10)$$

where $\delta t > 0$ is the arbitrary time increment. The phonon distribution function inside the thermal system is totally controlled by the boundary conditions or the phonon distribution function at $t = t_h$. Therefore, the local temperature cannot be smaller than the environment temperature based on Eq. (7). When the phonon N- or R- process scattering increases, the phonon transport can be approximately described by a hyperbolic heat conduction equation^{22,32,36,41,53},

$$c_1 \frac{\partial^2 T}{\partial t^2} + c_2 \frac{\partial T}{\partial t} + c_3 \nabla_{\mathbf{x}}^2 T = \dot{S}, \quad (11)$$

where c_1 , c_2 , c_3 are coefficients. When the N-process dominates, the heat wave term in Eq. (11) plays an important role on heat conduction^{22,36,53}. As reported in our previous paper⁴¹, as long as the heat conduction in thermal systems could be described by a hyperbolic equation and the wave term dominates, the temperature could fluctuate around the environment temperature within suitable initial and boundary conditions. That's a feature of the wave equation. It is not limited by the system size, dimensions and materials properties. When the R-process increases, the diffusion term dominates heat conduction so that the temperature fluctuation disappears.

In a word, the negative dimensionless temperature $(T_{probe} - T_0)/(T_h - T_0)$ could appear in two-dimensional materials. More importantly, different from the heat wave which can appear in both ballistic and hydrodynamic regimes³²⁻³⁴, this phenomenon could only appear in the phonon hydrodynamic regime, which is similar to what we have reported in three-dimensional materials⁴¹. Therefore, this phenomenon could be a unique macroscopic signature for the hydrodynamic phonon transport.

To make our conclusion more convincing, the heat conduction in a single-layer suspended graphene disk is studied due to its representativeness in two-dimensional materials^{18,36,54}, and the possibility of future experimental observations is discussed. The experimental parameters of dual-wavelength flash Raman mapping method^{43,44} provided by Dr. Aoran Fan are used: $L = 7 \mu\text{m}$, $r_{pump} = 259 \text{ nm}$, $r_{probe} = 282 \text{ nm}$ and $t_h = 20 \text{ ns}$. Note that $t_h = 20 \text{ ns}$ is long enough for sufficient phonon scattering and reaching steady-state. The phonon dispersion and polarization of graphene are calculated by the Vienna *Ab initio* Simulation Package (VASP) combined with phonopy. Details can be found in our previous paper⁴⁰. The physical nature of the photothermal conversion including photon-electron-phonon coupling is quite complicated^{47,50,55}, so that here we assume that all

phonons reach thermal equilibrium after absorbing the energy coming from heating laser beam⁴⁸ and the spectral weight is

$$G = \frac{C}{\sum_p \int C d\omega}. \quad (12)$$

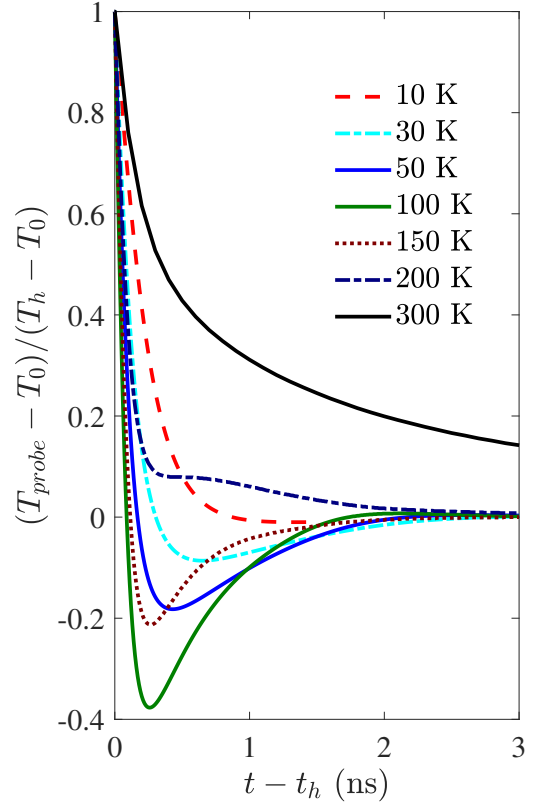


FIG. 3. The evolution of temperature in graphene disk under different environment temperature, where $t_h = 20 \text{ ns}$.

After the heat source is removed, the evolution of the probe temperature under different environment temperature are shown in Fig. 3. In room temperature, the heat dissipates gradually with time until reaching environment temperature. When the environment temperature decreases, the negative normalized temperature $(T_{probe} - T_0)/(T_h - T_0)$ is probed. Namely, the transient temperature could be smaller than the environment temperature. This phenomenon is quite obvious in the temperature range of 50 – 150 K. When the environment temperature further decreases, it can be observed that this phenomenon becomes weaker and weaker, and finally fades away at $T_0 = 10 \text{ K}$.

As reported in the previous studies^{18,20,36}, when the environment temperature decreases from high to extremely low temperature, the phonon transport in graphene could go through the diffusive, hydrodynamic and ballistic regimes in turn. In

other words, the negative dimensionless temperature phenomenon could appear in graphene disk and only appear in the hydrodynamic regime. It is consistent with those mentioned in 2D disk geometry.

V. CONCLUSION

In summary, a novel transient heat conduction in two-dimensional disk geometry is studied based on the phonon BTE under Callaway model. Using a heating pulsed Gaussian laser beam to heat the materials under the environment temperature, after the heat source is removed, the transient temperature could be lower than the environment temperature. This phenomenon could only appear in the hydrodynamic regime. Furthermore, by using the experimental parameters as the input of the phonon BTE, we found that this phenomenon could appear in a single-layer suspended graphene disk with diameter $7\ \mu\text{m}$ in the temperature range of $50 - 150\ \text{K}$. This work provides theoretical guidance for experimentally proving the existence and uniqueness of hydrodynamic phonon transport in two-dimensional disk geometry in the future.

ACKNOWLEDGMENTS

This work is supported by National Natural Science Foundation of China (12147122) and the China Postdoctoral Science Founda-

tion (2021M701565). The authors acknowledge Dr. Aoran Fan, Rulei Guo and Yufeng Zhang for their enthusiastic guidance and help in the Raman/pump-probe experimental details and parameters, acknowledge Prof. Zhaoli Guo, Nuo Yang, Samuel Huberman and Jingtao Lü for communications on hydrodynamic phonon transport.

Appendix A: Numerical discretizations of the phase space

The spatial space is discretized with 201×201 or 401×401 uniform cells. The first-order upwind scheme is used to deal with the spatial gradient of the distribution function in the ballistic regime, and the van Leer limiter is used in the hydrodynamic and diffusive regimes. The time step is $\Delta t = \text{CFL} \times \Delta x / v_{\text{max}}$, where Δx is the minimum discretized cell size, CFL is the Courant–Friedrichs–Lewy number and v_{max} is the maximum group velocity. In the two-dimensional solid angle space, $\mathbf{s} = (\cos\theta, \sin\theta)$, where $\theta \in [0, 2\pi]$ is the polar angle. Due to symmetry, the $\theta \in [0, \pi]$ is discretized with the N_θ -point Gauss-Legendre quadrature. In graphene disk, 300 discretized frequency bands are considered^{34,40} and the mid-point rule is used for the numerical integration of the frequency space. For all cases, $N_\theta = 50$ and $\text{CFL} = 0.04 - 0.4$. The present discretizations of the phase space are enough for all phonon transport regimes according to our previous experience^{22,34,40,41}.

* zhangc33@sustech.edu.cn

[†] Corresponding author: wul@sustech.edu.cn

¹ H. O. jr., *Prandtl-Essentials of Fluid Mechanics*, 3rd ed., Applied Mathematical Sciences, Vol. 158 (Springer-Verlag New York, 2010).

² R. N. Gurzhi, *Sov. Phys.-Usp.* **11**, 255 (1968).

³ H. Beck, P. F. Meier, and A. Thellung, *Phys. Status Solidi A* **24**, 11 (1974).

⁴ A. Lucas and K. C. Fong, *Journal of Physics: Condensed Matter* **30**, 053001 (2018).

⁵ S. Lee and X. Li, in *Nanoscale Energy Transport*, 2053-2563 (IOP Publishing, 2020) pp. 1–1 to 1–26.

⁶ G. Chen, *Nat. Rev. Phys.* **3**, 555 (2021).

⁷ R. A. Guyer and J. A. Krumhansl, *Phys. Rev.* **148**, 778 (1966).

⁸ R. A. Guyer and J. A. Krumhansl, *Phys. Rev.* **148**, 766 (1966).

⁹ M. Chester, *Phys. Rev.* **131**, 2013 (1963).

¹⁰ J. A. Sussmann and A. Thellung, *Proc. Phys. Soc.* **81**, 1122 (1963).

¹¹ Y. Guo and M. Wang, *Phys. Rep.* **595**, 1 (2015).

¹² C. C. Ackerman, B. Bertman, H. A. Fairbank, and R. A. Guyer, *Phys. Rev. Lett.* **16**, 789 (1966).

¹³ T. F. McNelly, S. J. Rogers, D. J. Channin, R. J. Rollefson, W. M. Goubau, G. E. Schmidt, J. A. Krumhansl, and R. O. Pohl, *Phys. Rev. Lett.* **24**, 100 (1970).

¹⁴ H. E. Jackson, C. T. Walker, and T. F. McNelly, *Phys. Rev. Lett.* **25**, 26 (1970).

¹⁵ V. Narayanamurti and R. C. Dynes, *Phys. Rev. Lett.* **28**, 1461 (1972).

¹⁶ A. Koreeda, R. Takano, and S. Saikan, *Phys. Rev. Lett.* **99**, 265502 (2007).

¹⁷ D. D. Joseph and L. Preziosi, *Rev. Mod. Phys.* **61**, 41 (1989).

¹⁸ S. Lee, D. Broido, K. Esfarjani, and G. Chen, *Nat. Commun.* **6**, 6290 (2015).

¹⁹ S. Lee and L. Lindsay, *Phys. Rev. B* **95**, 184304 (2017).

²⁰ X.-P. Luo, Y.-Y. Guo, M.-R. Wang, and H.-L. Yi, *Phys. Rev. B* **100**, 155401 (2019).

²¹ M. Xu, *Phys. Lett. A* **404**, 127402 (2021).

²² M.-Y. Shang, C. Zhang, Z. Guo, and J.-T. Lü, *Sci. Rep.* **10**, 8272 (2020).

²³ D. Benin and H. J. Maris, *Phys. Rev. B* **18**, 3112 (1978).

²⁴ X. Li and S. Lee, *Phys. Rev. B* **97**, 094309 (2018).

- ²⁵ Y. Guo and M. Wang, Phys. Rev. B **96**, 134312 (2017).
- ²⁶ S. Huberman, R. A. Duncan, K. Chen, B. Song, V. Chiloyan, Z. Ding, A. A. Maznev, G. Chen, and K. A. Nelson, Science **364**, 375 (2019).
- ²⁷ Z. Ding, K. Chen, B. Song, J. Shin, A. A. Maznev, K. A. Nelson, and G. Chen, Nat. Commun. **13**, 285 (2022).
- ²⁸ V. Martelli, J. L. Jiménez, M. Continentino, E. Baggio-Saitovitch, and K. Behnia, Phys. Rev. Lett. **120**, 125901 (2018).
- ²⁹ Y. Machida, N. Matsumoto, T. Isono, and K. Behnia, Science **367**, 309 (2020).
- ³⁰ Y. Machida, A. Subedi, K. Akiba, A. Miyake, M. Tokunaga, Y. Akahama, K. Izawa, and K. Behnia, Sci. Adv. **4**, eaat3374 (2018).
- ³¹ A. Beardo, M. G. Hennessy, L. Sendra, J. Camacho, T. G. Myers, J. Bafaluy, and F. X. Alvarez, Phys. Rev. B **101**, 075303 (2020).
- ³² A. Beardo, M. López-Suárez, L. A. Pérez, L. Sendra, M. I. Alonso, C. Melis, J. Bafaluy, J. Camacho, L. Colombo, R. Rurali, F. X. Alvarez, and J. S. Reparaz, Sci. Adv. **7**, eabg4677 (2021).
- ³³ V. Chiloyan, S. Huberman, Z. Ding, J. Mendoza, A. A. Maznev, K. A. Nelson, and G. Chen, Phys. Rev. B **104**, 245424 (2021).
- ³⁴ C. Zhang, S. Huberman, and L. Wu, arXiv preprint arXiv:2111.01578 (2022).
- ³⁵ R. J. Hardy, Phys. Rev. B **2**, 1193 (1970).
- ³⁶ A. Cepellotti, G. Fugallo, L. Paulatto, M. Lazzeri, F. Mauri, and N. Marzari, Nat. Commun. **6**, 6400 (2015).
- ³⁷ C. Zhang, Z. Guo, and S. Chen, Int. J. Heat Mass Transfer **130**, 1366 (2019).
- ³⁸ C. Zhang, S. Chen, and Z. Guo, Int. J. Heat Mass Transfer **176**, 121282 (2021).
- ³⁹ A. Beardo, M. Calvo-Schwarzwälder, J. Camacho, T. Myers, P. Torres, L. Sendra, F. Alvarez, and J. Bafaluy, Phys. Rev. Applied **11**, 034003 (2019).
- ⁴⁰ C. Zhang, D. Ma, M. Shang, X. Wan, J.-T. Lü, Z. Guo, B. Li, and N. Yang, Mater. Today Phys. , 100605 (2022).
- ⁴¹ C. Zhang and Z. Guo, Int. J. Heat Mass Transfer **181**, 121847 (2021).
- ⁴² J. Jeong, X. Li, S. Lee, L. Shi, and Y. Wang, Phys. Rev. Lett. **127**, 085901 (2021).
- ⁴³ S. Xu, A. Fan, H. Wang, X. Zhang, and X. Wang, Int. J. Heat Mass Transfer **154**, 119751 (2020).
- ⁴⁴ A. Fan, Y. Hu, H. Wang, W. Ma, and X. Zhang, Int. J. Heat Mass Transfer **143**, 118460 (2019).
- ⁴⁵ J. Callaway, Phys. Rev. **113**, 1046 (1959).
- ⁴⁶ B.-D. Nie and B.-Y. Cao, Nanosc. Microsc. Therm. **24**, 94 (2020).
- ⁴⁷ G. Chen, *Nanoscale energy transport and conversion: A parallel treatment of electrons, molecules, phonons, and photons* (Oxford University Press, 2005).
- ⁴⁸ V. Chiloyan, S. Huberman, A. A. Maznev, K. A. Nelson, and G. Chen, Appl. Phys. Lett. **116**, 163102 (2020).
- ⁴⁹ C. Hua and A. J. Minnich, Phys. Rev. B **97**, 014307 (2018).
- ⁵⁰ A. K. Vallabhaneni, D. Singh, H. Bao, J. Murthy, and X. Ruan, Phys. Rev. B **93**, 125432 (2016).
- ⁵¹ Z. Ding, J. Zhou, B. Song, V. Chiloyan, M. Li, T.-H. Liu, and G. Chen, Nano Lett. **18**, 638 (2018).
- ⁵² Z. Guo and K. Xu, Adva. Aerodyn. **3**, 6 (2021).
- ⁵³ M. Simoncelli, N. Marzari, and A. Cepellotti, Phys. Rev. X **10**, 011019 (2020).
- ⁵⁴ X. Gu, Y. Wei, X. Yin, B. Li, and R. Yang, Rev. Mod. Phys. **90**, 041002 (2018).
- ⁵⁵ C. Deng, Y. Huang, M. An, and N. Yang, Mater. Today Phys. **16**, 100305 (2021).